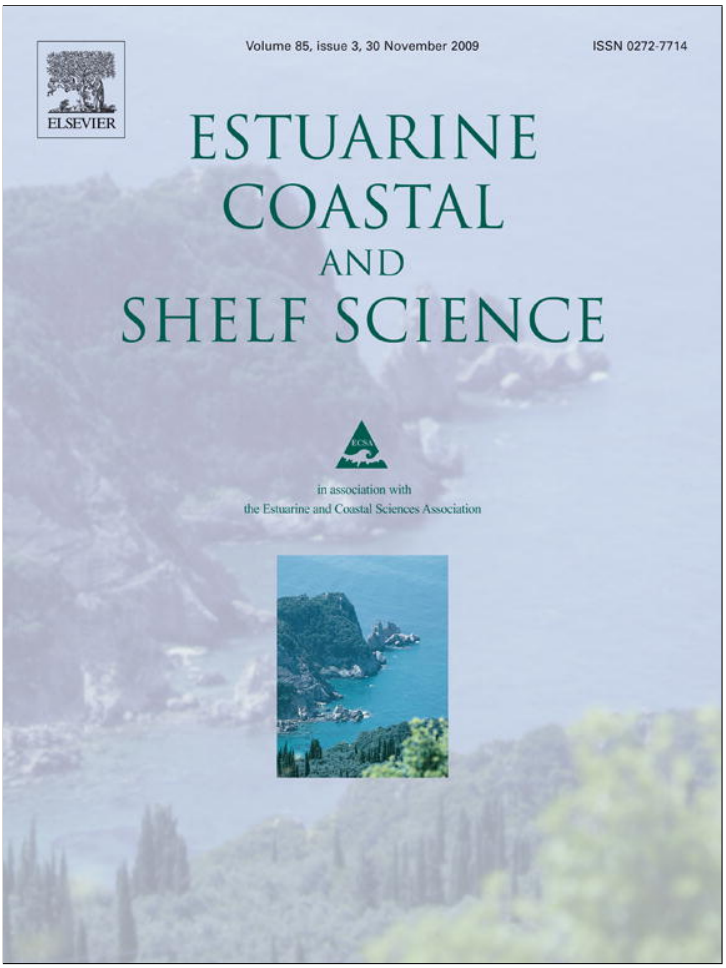

Estuarine, Coastal and Shelf Science 85 (2009) 487–496

Contents lists available at ScienceDirect

Estuarine, Coastal and Shelf Science

journal homepage: www.elsevier.com/locate/ecss

Three-dimensional distribution of larval fish assemblages across a surface thermal/chlorophyll front in a semienclosed sea

A. Danell-Jiménez [a], L. Sánchez-Velasco [a,*], M.F. Lavín [b], S.G. Marinone [b]

[a] Centro Interdisciplinario de Ciencias Marinas. Av. Instituto Politécnico Nacional s/n. Col. Playa Palo de Sta. Rita. La Paz, B.C.S. 23000, Mexico
[b] Centro de Investigación Científica y de Educación Superior de Ensenada, Km. 107, Carretera Tijuana-Ensenada, Ensenada, Baja California 22860, Mexico

ARTICLE INFO

Article history:
Received 23 January 2009
Accepted 10 September 2009
Available online 26 September 2009

Keywords:
larval fish assemblages
zooplankton biomass
thermal/chlorophyll front
México
Gulf of California

ABSTRACT

The oceanographic processes involved in marine fronts and their effects on the plankton are still a challenge in the understanding of marine ecosystems. This study examines the relationship of the three-dimensional distribution of larval fish assemblages (LFAs) with hydrography on a tidal-mixing surface thermal/chlorophyll front in the highly productive midriff archipelago of the Gulf of California during summer (August, 2005). Zooplankton samples were obtained on both sides of the front with an opening–closing net (505 μm) in 50-m strata from the surface to 200 m depth. The Bray–Curtis dissimilarity index defined three strata groups with different LFAs. On the cool side of the front, characterized by high chlorophyll, salinity, and dissolved oxygen, an LFA with the lowest larval abundance (97 larvae/10 m^2) and low taxa number (44) was defined. On the warm side of the front, where the lowest concentrations of surface dissolved oxygen and surface chlorophyll were recorded, an LFA was defined on the pycnocline, with the highest mean larval abundance and number of taxa (927 larvae/10 m^2 and 109 taxa); it was composed of epipelagic, mesopelagic, and demersal species. Also on the warm side of the front, but below the pycnocline, an LFA was observed with medium larval abundance and taxa number (126 larvae/10 m^2 and 28 taxa), formed by mesopelagic species. This assemblage was absent from the cool area to the northwest of the front, mainly from 150 to 50 m depth, where maximum-salinity water from the Northern Gulf was found. We conclude that the surface thermal/chlorophyll front had a profound effect on LFAs distribution in the surface layer, while the southward intrusion of maximum-salinity water from the Northern Gulf bounded the LFAs distribution in the deeper layer under the pycnocline. Therefore, in addition to the surface thermal/chlorophyll front, the hydrographic processes associated with the Gulf's seasonal and thermohaline circulation affect the LFAs three-dimensional distribution. Similar relationships may occur in other ocean ecosystems.

1. Introduction

Mesoscale hydrographic structures such as eddies and fronts may act as mechanisms that concentrate or disperse planktonic organisms, and therefore contribute to increase the spatial heterogeneity of fish eggs and larvae and other planktonic organisms (Sournia, 1994; Okazaki and Nakata, 2007).

Relationships between larval fish assemblages and hydrographic features such as fronts have been documented in different periods and geographic regions of the world. For example at the Ensenada front in the California Current region, Moser and Smith (1993) found that primary productivity was higher in the colder area north of the front than in the area to the south, and zooplankton biomass was highest at the front, remarking that the vertical distribution of fish larvae was a function of pycnocline depth. In the Catalan Sea (Northwestern Mediterranean), Sabatés and Olivar (1996) analyzed the variation in larval fish distributions associated with a shelf–slope salinity front. They found that offshore dispersal of fish larvae of shelf-dwelling species was limited by the geographical position of the front. For the tidal front around Georges Bank, Wishner et al. (2006) found the highest concentrations of zooplankton biomass on the oceanic stratified side of the front, and the largest fish larvae concentrations in the upper 40 m of the shallow well-mixed side of the front. These studies showed different relationships between the zooplankton and different kinds of fronts; the understanding of these relationships is still a challenge in marine ecology.

In the Gulf of California (Insert, Fig. 1a), an oceanographically complex body of water (see review by Lavín and Marinone, 2003), the presence of surface thermal fronts (Figs.1b and 2a,c) to the north

* Corresponding author.
E-mail addresses: anelldaji@yahoo.com.mx (A. Danell-Jiménez), lsvelasc@gmail.com (L. Sánchez-Velasco), mlavin@cicese.mx (M.F. Lavín), marinone@cicese.mx (S.G. Marinone).

0272-7714/$ – see front matter © 2009 Elsevier Ltd. All rights reserved.
doi:10.1016/j.ecss.2009.09.010

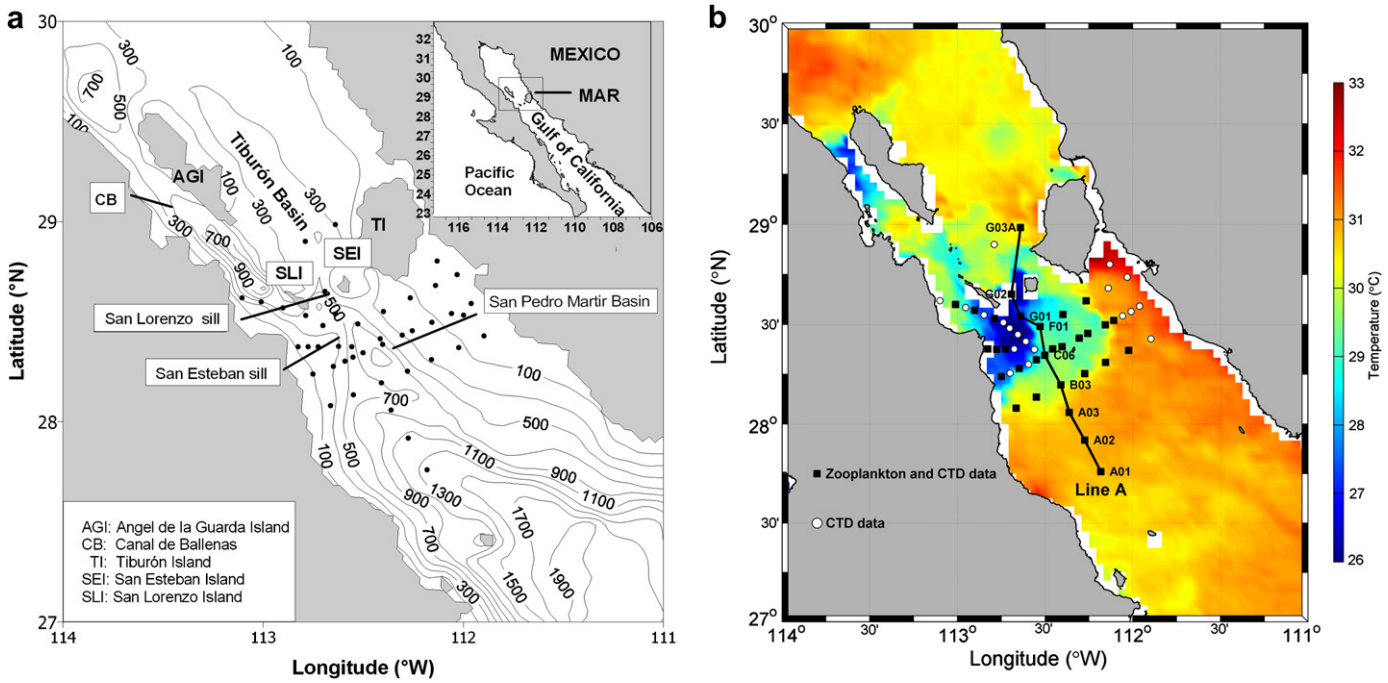

Fig. 1. (a) Bathymetry of the midriff archipelago region (MAR) of the Gulf of California, and named islands, channels and sills. Dots are sampling stations; (b) Sea-surface temperature image (GOES) from August 14, 2005, with grid of stations: Black squares (■), CTD and zooplankton data. White circles (○), CTD data only.

and south of the midriff archipelago region is well documented from satellite images (Paden et al., 1991). The reason for the presence of these fronts is the weakening of stratification by the turbulent kinetic energy released during the passage of the semidiurnal tidal wave through the constrictions of the archipelago (Argote et al., 1995; Marinone and Lavín, 2003), especially over the San Lorenzo and San Esteban sills. Together with the cool water, tidal mixing brings nutrients to the surface layers, causing an increase of phytoplankton in the front and in the cool area and, consequently, the formation of sharp surface chlorophyll fronts, which are also evident in satellite images (Fig. 2b,d). These processes make the midriff archipelago region one of the most productive regions of the Gulf of California (Álvarez-Borrego and Lara-Lara, 1991).

Studies focusing on relationships of larval fish assemblages with hydrographic structures in the Gulf are scarce. Some authors have associated the distribution of fish eggs and larval fish assemblages with sea-surface temperature (SST), by using temperature measured *in situ* or from satellites (e.g., Green-Ruiz and Hinojosa-Corona, 1997; Avalos-García et al., 2003), showing spatial changes in the larval fish distributions associated with changes in SST. In addition, Sánchez-Velasco et al. (2006) in the southwestern Gulf and Peguero-Icaza et al. (2008) in the northern Gulf found correlation between larval fish assemblages and circulation; and Sánchez-Velasco et al. (2007) found that the highest larval fish concentration in the water column was associated with the maximum stability layer. However, there are no detailed studies on relationships of plankton organisms in general, or of fish larvae in particular, with hydrographic structures such as fronts and eddies.

In this study we investigate the three-dimensional distribution of larval fish assemblages around the surface thermal/chlorophyll front located south of the midriff archipelago, and its relationship with the hydrography and the circulation.

2. Methods

Physical and zooplankton data were obtained from the *R/V Francisco de Ulloa*, from 11 to 16 of August 2005, on the 32 stations shown in Fig. 1. Temperature and conductivity profiles were obtained at each station with a SeaBird 911*plus* CTD (conductivity, temperature and depth profiler), including recently-calibrated dissolved oxygen and fluorescence sensors. Chlorophyll concentration was calculated from the fluorescence; although chlorophyll samples were taken at the surface and at the subsurface maximum, we present here only the fluorescence-derived chlorophyll. The geopotential anomaly, which reflects the height of the sea-surface topography and hence the geostrophic circulation (cyclonic flow around lows, anticyclonic flow around highs), was calculated from objectively-mapped potential temperature (θ) and salinity (S) distributions by integrating the specific volume anomaly upward from the reference level. A standard objective-mapping interpolation was used, with a classic Gaussian correlation function with relative errors of 0.1, a 50-km horizontal length scale and a 70-m vertical scale.

The section named "A" (Fig. 1b) was selected from the grid in order to describe the hydrographic structure of the water column and to relate it with biological data. It was approximately aligned with the axis of the Gulf of California, and it crossed the frontal area over San Esteban sill. The grid of stations was designed with the aid of chlorophyll and SST images from the MODIS satellites (4 km × 4 km resolution), obtained from http://oceancolor.gsfc.nasa.gov/cgi/level3.pl. Surface temperature images were also obtained from the GOES satellites (6 km × 6 km) (http://sgiot2.ssd.nesdis.noaa.gov/data_drive/products/goes/tiff).

Lagrangian surface currents were measured with two surface drifters with 10 m Holey socks centered at 15 m, and tracked with the ARGOS satellite telemetry system. The data were quality-controlled and interpolated at 6-hour intervals by the Global Drifter Program of NOAA, as prescribed by Hansen and Poulain (1996).

As an aid in the discussion of the results, use was made of outputs from a 3D baroclinic numerical model of the Gulf of California, which has been documented by Marinone (2003). The model domain is the entire Gulf, and the version used here has a mesh size of 0.833′ × 0.833′ (~1.31 × 1.54 km) in the horizontal and 12 layers in the vertical. It was forced at the entrance with

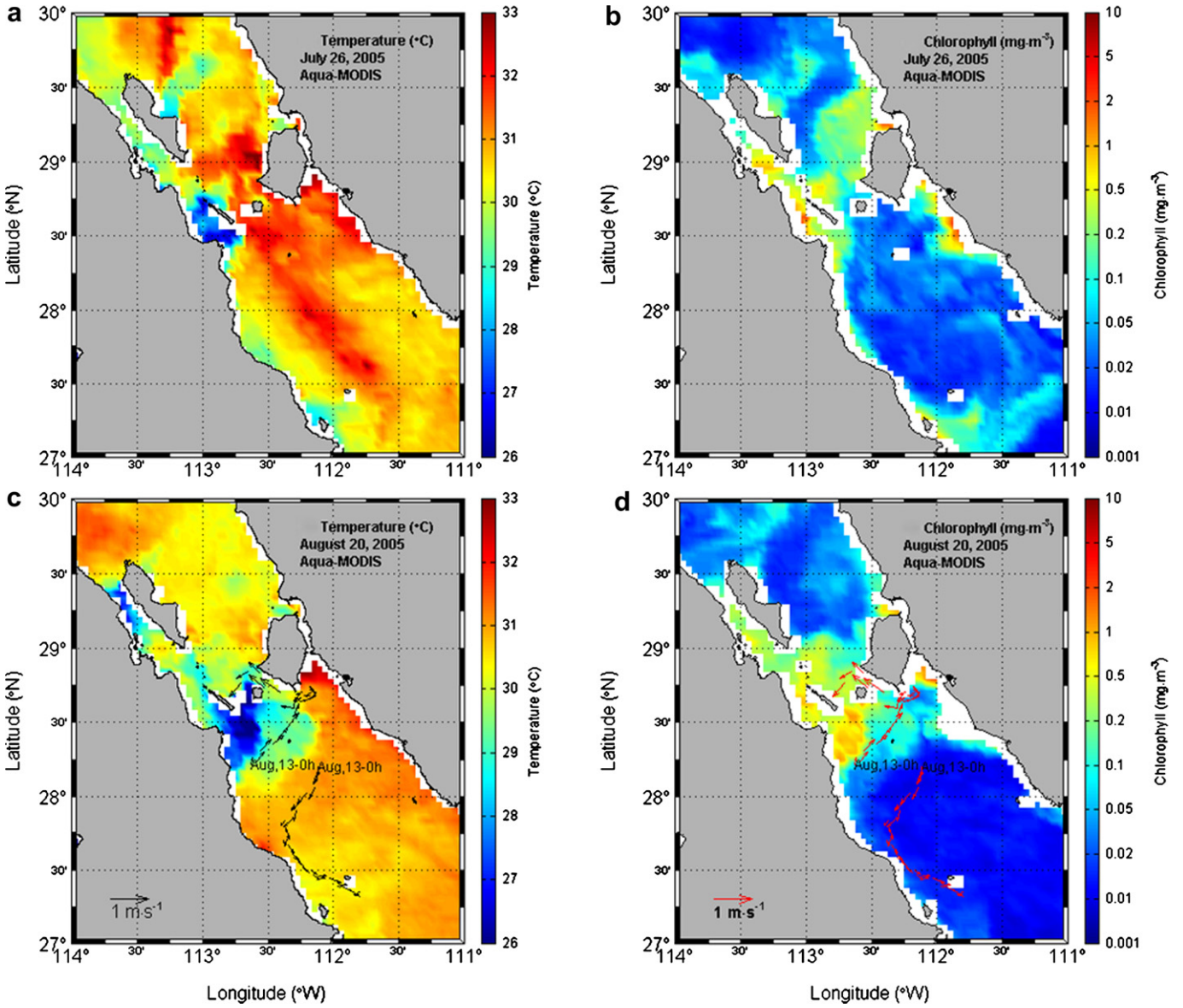

Fig. 2. Thermal and chlorophyll MODIS images before and after the survey. (a) Thermal image, July 26, 2005. (b) Chlorophyll image, July 26, 2005. (c) Thermal image, August 20, 2005. (d) Chlorophyll image, August 20, 2005. The arrows in the last two images are the 6-hourly tracks and velocities of two satellite-tracked surface drifters, starting on August 13 at 00:00 h (UT). The images are 7-day averages, centered on the dates shown.

seven tidal harmonics and with the climatological annual variability of hydrography, and at the surface with a sinusoidal up–down–gulf wind of annual period.

Oblique zooplankton hauls were made during day and night hours at four depths in the water column from 200 to 150 m, from 150 to 100 m, from 100 to 50 m, and from 50 to the surface, using opening-closing conical zooplankton nets, with a mouth diameter of 50 cm, 250 cm of net length and 505 μm mesh size (http://www.generaloceanics.com/genocean/1000DT.htm). The closed net was lowered to the bottom of the stratum to be sampled, then it was opened with a manual brass messenger, and the haul was started. When the upper level of the sampling stratum was reached, the net was closed with another messenger and the haul terminated. This system effectively avoids contamination of the sample with organisms from other strata. This closing system was very precise, since it responded almost instantaneously for surface hauls (50 m to surface), while the maximum delay was 10 s for the deepest hauls (150–200 m). Two strata were sampled in each haul, and hauls were repeated for nets that were tangled in any way when surfacing. The depth for each stratum was calculated by the cosine of the wire angle method following the standard specifications of Smith and Richardson (1979). This stratified sampling technique has been used successful in previous studies (e.g., Espinosa-Fuentes and Flores-Coto, 2004; Sánchez-Velasco et al., 2007).

The volume of filtered water was calculated using calibrated flow meters placed in the mouth of each net. Samples were fixed with 5% formalin buffered with sodium borate. Zooplankton biomass, estimated by displacement volume (Kramer et al., 1972), was standardized to mL/1000 m^3. Fish larvae were removed from the samples and identified according to the descriptions in Moser (1996). Fish larvae abundance was standardized to number of larvae per 10 m^2 (Smith and Richardson, 1979), which are the usual units for larval abundance in the open sea (e.g., Moser and Smith, 1993).

The non-parametric Kruskal–Wallis test (Sokal and Rohlf, 1985; Siegel and Castellón, 1988) was used to assess the statistical significance of differences of the total larval abundance between day and night hours and among the different depth strata. When the null hypothesis was rejected, Dunn's multiple comparison test was used for establishing whether significant differences occurred in pairs of strata (Siegel and Castellón, 1988).

Similarities among the different depth strata were based on taxa with a frequency of occurrence $\geq$5% in each period. The standardized data were fourth-root transformed. Planktonic habitats or groups of strata were defined using the Bray–Curtis dissimilarity index, a technique that is not affected by multiple absences and gives more weight to abundant species than to rare ones (Bray and Curtis, 1957; Field et al., 1982). Dendrograms were made by the flexible agglomerative clustering method (Sokal and Sneath, 1963).

The set of species identified in each planktonic habitat was considered as an LFA. Some species can be present in various habitats because the premise is that although adult fish cross planktonic boundaries, their eggs and larvae might be retained (e.g., Espinosa-Fuentes and Flores-Coto, 2004; Sánchez-Velasco et al., 2007). If the habitats are favorable for their survival, the larvae would develop in the different habitats during their planktonic phase. The difference in larval abundance is expected to show the main spawning area of the species.

The dominant species of each LFA were obtained in accordance with the Olmstead–Tukey test (Sokal and Rohlf, 1985), which takes into account the abundance and relative frequency of each species. The dominant species were considered as the representative species of each LFA.

3. Results

3.1. Hydrography

The grid of stations covered both sides of the thermal frontal area (Fig. 1b). Although there were no chlorophyll images for the days of the survey (because of clouds), the chlorophyll satellite images from before and after the cruise (Figs. 2b and 2d) indicate that the cool area was probably chlorophyll-enriched at the time of the cruise. Furthermore, the *in situ* surface data (Fig. 3) showed that the surface in the cool area (Fig. 3a) contained more chlorophyll (Fig. 3c) than the warm area to the southeast. The SST presented differences of up to 3 °C, from 27 °C in the cool side of the front to 30 °C in the warm side to the south and southeast (Fig. 3a). The sharpest across-front surface thermal contrast was relatively modest at ~1.5 °C, and the SST front was less than 10 km wide. The surface salinity (Fig. 3b) was higher in Ballenas Channel (35.3–35.2) than to the southeast (~35.1), but there was no strong haline surface front associated with the SST front. The surface dissolved oxygen (Fig. 3d) had a maximum that coincided with the chlorophyll maximum (Fig. 3b). The across-front change in dissolved oxygen was from 4.7 to 4.0 mL/L, while that in chlorophyll was from 0.7 to 0.1 mg m^{-3}.

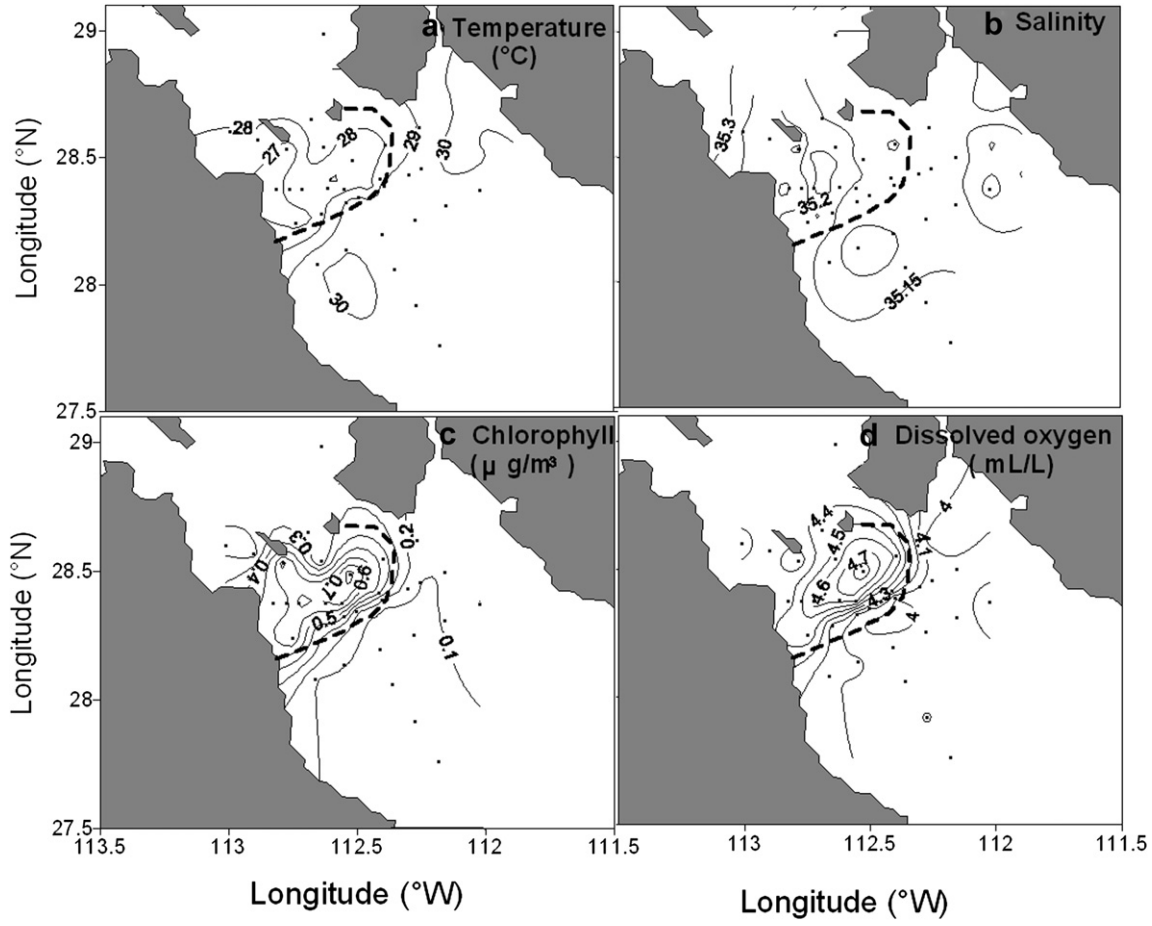

Fig. 3. Average values in the top 10 m of the water column of hydrographic variables from the CTD: (a) Potential temperature (°C), (b) Salinity, (c) Chlorophyll (mg m^{-3}), (d) Dissolved oxygen (mL/L). The dashed line is the thermal front drawn from the GOES thermal image shown in Fig. 1.

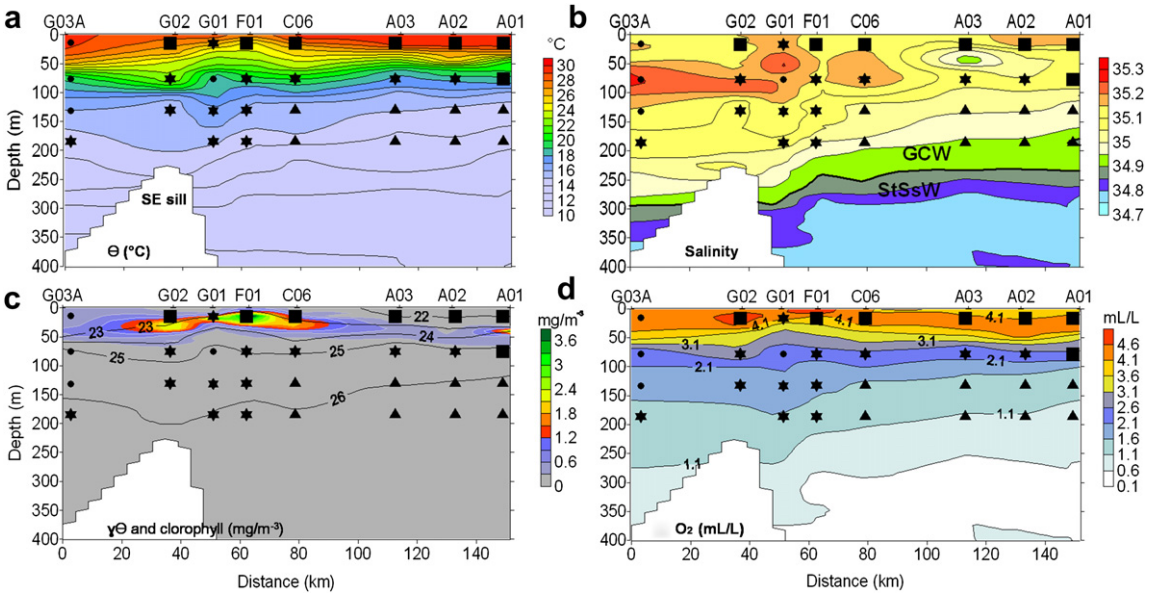

Fig. 4. Vertical distributions along line A: (a) Potential temperature (°C), (b) salinity, (c) potential density anomaly (γ_θ, isolines) and chlorophyll (color map, mg m^{-3}), (d) dissolved oxygen (mL/L). In (c): StSsW means Subtropical Sub-surface Water, GCW means Gulf of California Water. Symbol code for larval fish assemblages: Squares (■),Warm-frontal. Stars (★), Cool-frontal. Triangles (▲), Deep. Small dots (●), samples without fish larvae.

The subsurface hydrographic structure on the along-Gulf line of stations (marked A in Fig. 1b) is shown in Fig. 4. Thermal stratification was very strong and continuous from 16 °C at ~120 m to 29 °C at the surface in the two extremes of the section (Fig. 4a). In the frontal zone above the sill, the isotherms from 19 to 29 °C were domed, but only the 28 °C isotherm intersected the surface, rising from ~40 m outside the cool area (Figs. 3a and 4a). The weakness of the front was probably due to the fact that in August (and September) the Gulf of California shows its highest SST and therefore its strongest stratification. The surface mixed layer depth, defined as the depth where temperature was 0.5 °C lower that at the surface, was ~20 m deep at the two ends of the section, while it was a couple of meters deep at the front. Although some of the undulations of the isotherms were probably associated with internal hydrodynamics, the individual profiles (not shown) also suggested internal mixing below the frontal area.

The salinity distribution (Fig. 4b) shows a core of maximum-salinity water (35.1–35.2) in the 50–150 m layer. The figure suggests that the maximum-salinity water is an intrusion from the northern Gulf, which is the only possible source of sub-surface water of such high salinity, The core was immersed in Gulf of California Water ($S > 34.9$) seen in the upper 300 m in Fig. 4b, above the Subtropical Subsurface Water.

The isopycnal distribution (Fig. 4c) showed a surface density front between stations C06 and A03 which could be a barrier to the horizontal transfer of properties (e.g. temperature, fish larvae) between the cold and warm sides of the front. The distribution of chlorophyll on the potential density anomaly γ_θ (Fig. 4c) shows that the maximum chlorophyll concentration was under the surface, in a 40-m thick band centered on the $\gamma_\theta = 23$ isopycnal, which raised from ~40 m away from the cool area to near the surface over the sill (Fig. 4c). The dissolved oxygen was maximum in the surface layer and diminished with depth (Fig. 4d).

3.2. Currents

The surface currents revealed by the two surface drifters deployed during the cruise are shown in Fig. 2c,d, overlain on the SST and chlorophyll images of August 20. The drifter in the southern, warm side first traveled to the southwest (~30 cm s^{-1}) parallel to the front, and then turned to the southeast. The drifter deployed on the cold side first traveled to the northeast parallel to the front, and after being trapped for a couple of days south of Tiburón Island, it made a cyclonic (anticlockwise) half-turn around San Esteban Island.

The dynamic height relative to 100 m (Fig. 5) shows a low on the cool area and a high on the warm area resulting in cyclonic geostrophic flow in the former and anticyclonic geostrophic flow

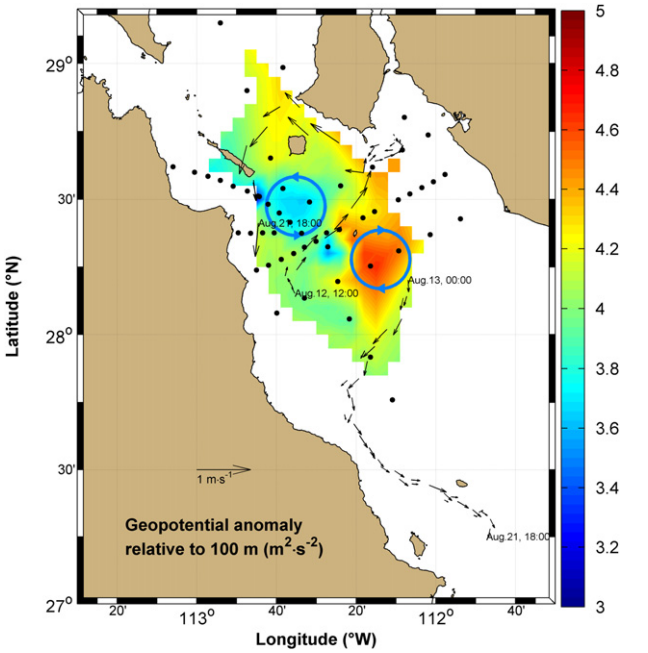

Fig. 5. Geopotential anomaly (m^2 s^{-1}) relative to 100 m, calculated from the CTD data. The thin arrows are the velocities of the surface drifters: the start and end date are shown. The thick blue arrows indicate the geostrophic velocity direction.

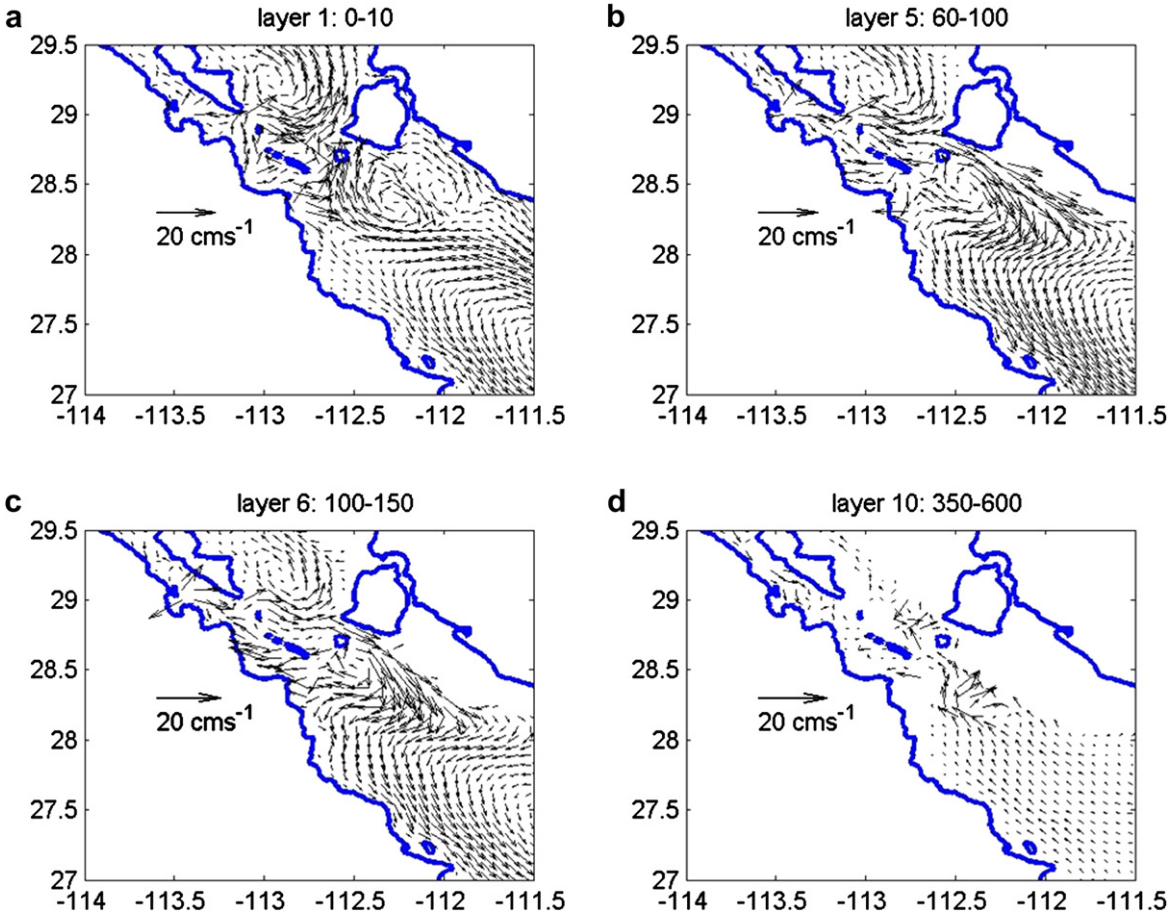

Fig. 6. Monthly average for August of the horizontal current fields predicted by the 3D numerical model of Marinone (2003) for layers (a) 0–10 m, (b) 60–100 m, (c) 100–150 m, and (d) 350–600 m. For clarity, only one every 5 vectors is shown.

in the latter; this flow pattern is indicated by the thick blue arrows in Fig. 5. The northeastward geostrophic flow on the frontal area seems to have been followed by the northern drifter.

Fig. 6 shows the monthly average for August of the horizontal current fields predicted by the numerical model for the layers 0–10 m, 60–100 m, 100–150 m, and 350–600 m. The agreement of the surface circulation with the northeastward trajectory of the northern drifter in the deep area (Fig. 2c,d) is quite good. The flow around the sills and smaller islands is complex, and not necessarily reflected by this drifter. The overall summer cyclonic circulation of the southern Gulf, shown by the model in Fig. 6a,b, seems to have been followed by the southern drifter.

3.3. Zooplankton biomass

The highest values of zooplankton biomass (>300 mL/1000 m^3) were located in the surface level (50 m to the surface) in the cool zone adjacent to front and in the warm side of the front (Fig. 7a). These values decreased with depth in all sampling stations, except in some stations under the SST frontal area, where relatively high biomass values were recorded in the 50–100 m and 100–150 m strata (Fig. 7b,c).

3.4. Fish larvae

There were no statistically significant differences in the total larval abundance between day and night hours in all cases ($P > 0.05$). However, there were significant differences in the total larval abundance among the four strata ($P > 0.05$) (Table 2); the surface stratum contained the highest abundance, while the deepest stratum had the lowest abundance.

Of a total of 5779 fish larvae identified in the study, *Benthosema panamense* larvae were the most abundant in the four strata (>70% of the total larval abundance of each stratum) (Table 1); and *Syacium ovale*, *Triphoturus mexicanus,* and *Albula* sp. larvae were relatively abundant throughout the water column. In all cases, the larval abundance decreased with the depth.

The Bray–Curtis dissimilarity Index defined three planktonic habitats, with LFAs that differed in composition and abundance at a level near one (Annex 1). They were named as follows: Warm-frontal LFA, Cool-frontal LFA and Deep LFA (Fig. 8).

The Warm-frontal LFA had 109 taxa and mean abundance of 927 larvae/10 m^2. This LFA was observed in the entire water column (squares, Fig. 8), but was mainly concentrated in the 0–50 m stratum of the warm area to the southeast of the front (squares, Fig. 8a); it was also found in a few surface samples in the cool side of the front. It was dominated by species of different adult habitats, such as *Albula* sp. (shallow demersal), *Auxis* sp. (epipelagic), *B. panamense* (mesopelagic), Carangidae T1, *Harengula thrissina* and *Selar crumenophthalmus* (coastal pelagics), *S. ovale* and *Cyclopsetta panamensis* (shallow demersal), and *T. mexicanus* (mesopelagic) (Table 3).

The Cool-frontal LFA had lower number of taxa (44) and lower mean larval abundance (97 larvae/10 m^2) than the Warm-frontal LFA. It was also found in the entire sampled water column, but it was clearly prevalent in the cool zone to the

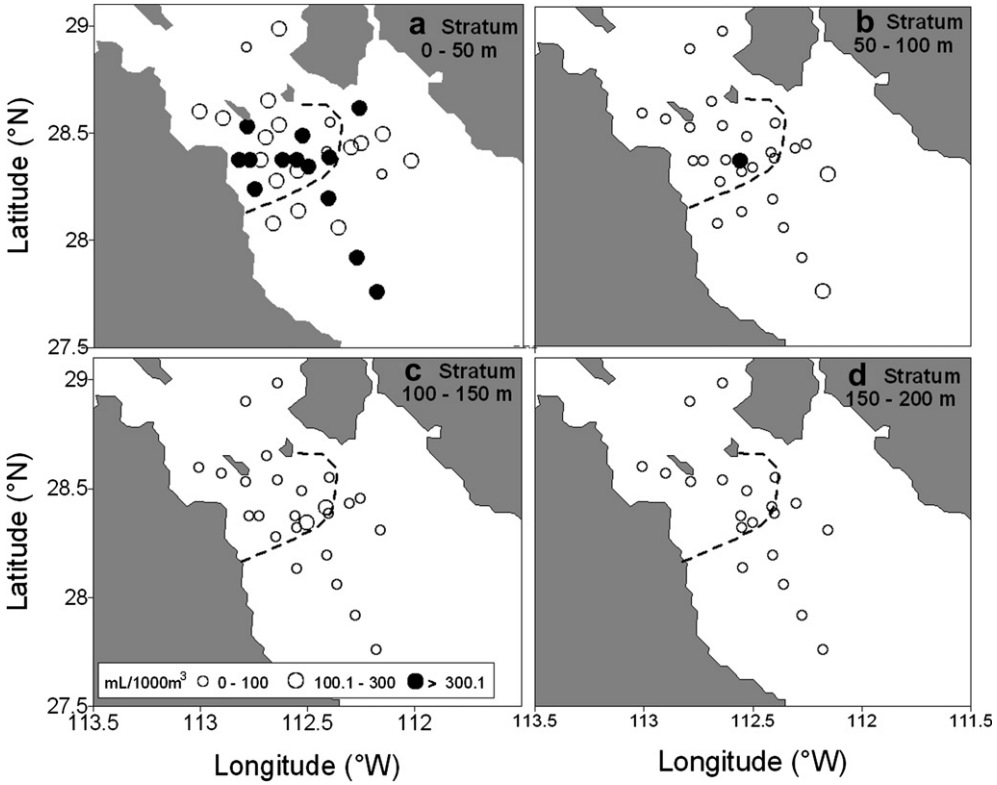

Fig. 7. Distribution of zooplankton biomass (mL/1000 m^3), by depth strata, in the midriff archipelago region of the Gulf of California (August 2005). The dashed line is the surface thermal front drawn from the GOES thermal image shown in Fig. 1.

northwest of the front (stars, Fig. 8). In the 50–100 m stratum, this assemblage seemed to concentrate closer to the front than in the other strata. *B. panamense* was the dominant species, which was associated to the shallow demersal species *Albula* sp. and Gobiidae T7, but in lower abundance and frequency than the former (Table 3).

The Deep LFA had a mean abundance of 126 larvae/10 m^2, and had the lowest number of taxa (28). It was located mainly deeper than 50 m in the warm side to the southeast of the front (triangles, Figs. 8c,d). The mesopelagic *B. panamense* and *V. lucetia* were the dominant species (Table 3).

The samples in which fish larvae were absent, shown as dots in Fig. 8, were found almost exclusively in the 50–100 m stratum of the cool area. They coincided with the high-salinity intrusion in that layer apparent in Fig. 4b.

3.5. Fish larvae and vertical hydrographic structure

The overlay of the LFAs on the vertical hydrographic sections along Line A (Fig. 4) complements the description above. The Warm-frontal LFA (squares, Fig. 4) was found in the warm side of the front, mainly in the first 50 m; however, it was also found in a few samples from the surface on the cool side. The Cool-frontal LFA (stars, Fig. 4) was dominant in the layers below 50 m of the cool side; the only samples in this part that were not classified as Cool-frontal LFA were those without larvae (dots, Fig. 4). This assemblage was also found at the top stratum of station G01, and in the 50–100 m stratum on the warm side. The Deep LFA (triangles, Fig. 4) was found exclusively from 100 to 200 m depth in the southeast area. The subsurface maximum-salinity tongue (Fig. 4b) appears to be a boundary between the Cool-frontal and Deep assemblages from 50 to 200 m depth.

4. Discussion

4.1. Front-fish larvae relationships in the Gulf of California

Although the surface thermal-chlorophyll front over the southern sills of the midriff archipelago has been observed via satellite images for some time (e.g., Paden et al., 1991; Santamaría-del-Angel et al., 1994), its detailed hydrographic structure has been studied very little, and its effects on the zooplankton community even less. This is the first interdisciplinary study that seeks to establish front-fish larvae relationships by direct observation in the most productive region of the Gulf of California.

While most tidal-mixing fronts are found in shallow waters in continental shelves, the front under study is found in deep water (Simpson et al., 1994). This is why there are no vertically well-mixed conditions, which is in agreement with the calculations of tidal energy dissipation rate in the Gulf made by Argote et al.

Table 1
Dominant species per stratum of depth in the midriff archipelago region of the Gulf of California (August 2005). %F:, percentage of occurrence. X: mean abundance. Abundance is expressed as number of larvae per 10 m^2.

	0–50 m		50–100 m		100–150 m		150–200 m	
Dominant species	X	%F	X	%F	X	%F	X	%F
Albula spp.[a]	6.4	39	5.2	10	1.7	5	9.0	17
Auxis spp.[b]	12.9	52	1.6	10	1.3	5	2.4	11
Benthosema panamense[c]	678.4	100	194.8	95	112.1	95	123.3	83
Syacium ovale[a]	12.0	39	4.0	10	10.4	30	4.7	6
Triphoturus mexicanus[c]	8.6	36	15.4	45	6.0	40	8.3	28

[a] Shallow demersal.
[b] Epipelagic.
[c] Mesopelagic.

Table 2
a) Mean ranges of the non-parametric Kruskall–Wallis test applied to the larval fish abundance per stratum of depth in the midriff archipelago region of the Gulf of California (August 2005). b) Results of the Dunńs multiple comparison test establishing in which pairs of strata significant differences occurred.

a)	Stratum 1	Stratum 2	Stratum 3	Stratum 4	Test	Probability	Significance level
Strata number	14	11	9	5			
Mean ranges	28.6	15.4	15.3	14.4	12.6	0.006	$P < 0.05$
b)	Stratum 1	Stratum 2	Stratum 3				
Stratum 2	*0.2158						
Stratum 3	*0.4335	*0.4335					
Stratum 4	*0.4060	*0.4060	*0.4060				

* Significant differences at 95%.

(1995). Marinone and Lavín (2003) and Mateos et al. (2006) suggested that geostrophic flows could be generated by the distortion of the density field caused by the turbulent processes over and around the sills. The dynamic height (Fig. 5) and the drifter tracks (Fig. 2c,d) are probably the first observational evidence of this, and they suggest that surface particle trapping could occur in the cool area. Trapping of larvae in this area was also found by Peguero-Icaza et al. (2008).

We found that the hydrographic contrasts between the two sides of the front, and the associated circulation, generated different planktonic habitats which were reflected in the three-dimensional distribution of the three LFAs defined in this study.

The Cool-frontal assemblage, which had the lowest larval abundance and number of taxa, was found on the intense-mixing area over the sills and in Ballenas Channel, where the lowest temperature and high salinity, high dissolved oxygen and high chlorophyll were recorded. The basic reason for these environmental conditions is the intense vertical mixing caused by the turbulent kinetic energy extracted from the tidal wave as it accelerates past the sills: cool, nutrient-rich water is continuously brought to the euphotic zone, causing the maximum surface chlorophyll observed in our *in situ* data (Fig. 3c) and in the satellite images (Álvarez-Borrego and Lara-Lara, 1991; Santamaría-del-Angel et al., 1994). However, the strong vertical mixing also carries the phytoplankton away from the euphotic zone for a fraction of the time, which conditions the phytoplankton to low irradiances and reduces the capacity for photosynthesis, causing the primary productivity to be lower than in the well-stratified southern Gulf (Cortés-Lara et al., 1999).

We consider that the low larval abundance in this planktonic habitat may also be due to the continuous and intense vertical mixing, which produces low stability by weakening the pycnocline (Argote et al., 1995; Marinone and Lavín, 2003; Sánchez-Velasco et al., 2009), and by the relative isolation of the cool area suggested by the dynamic height and the current observations (Fig. 5). Authors such as Avalos-García et al. (2003) and Sánchez-Velasco et al. (2004) had speculated that these conditions were unfavorable for the survival of fish larvae, but their sampling stations were not close enough to resolve the frontal area.

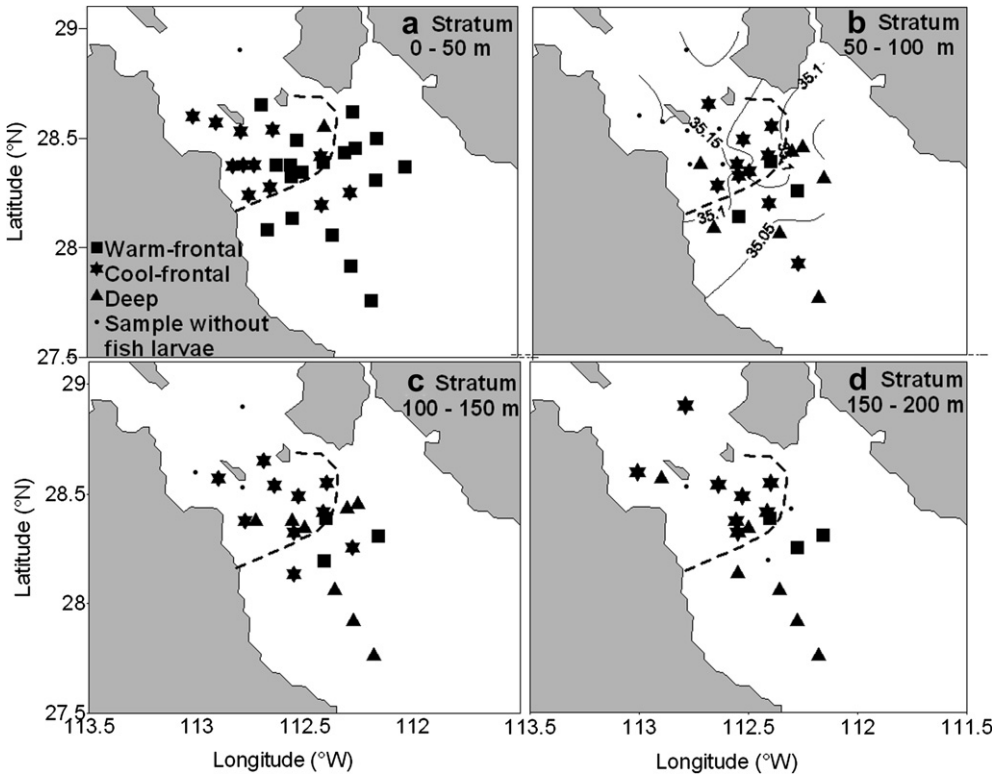

Fig. 8. Distribution by strata of the larval fish assemblages in the midriff archipelago region of the Gulf of California (August 2005): (a) 0–50 m, (b) 50–100 m, (c) 100–150 m, (d) 150–200 m. The dashed line is the thermal front drawn from the GOES thermal image shown in Fig. 1. Symbol code for larval fish assemblages: Squares (■), Warm-frontal. Stars (★), Cool-frontal. Triangles (▲), Deep. Small dots (●), sample without fish larvae.

Table 3

	Warm-frontal		Deep		Cool-frontal	
Dominant species	X	%F	X	%F	X	%F
Albula spp.	5.3	50.0				
Auxis spp.	34.2	64.3				
B. panamense	14.2	100.0	103.1	76.2	84.6	100.0
Carangidae T1	6.6	35.7				
Cyclopsetta panamensis	5.8	21.4				
Harengula thrissina	8.4	14.3				
Selar crumenophthalmus	7.1	14.3				
Syacium ovale	3.8	60.7				
Triphoturus mexicanus	14.7	42.9				
Vinciguerria lucetia			54.12	14.29		
Species		109		28		44
Mean abundance		926.8		126.0		96.9
Station/stratum		28		21		41

The Warm-frontal assemblage, which was dominated by larvae of adults of diverse environments such as epipelagic (*Auxis* spp.), mesopelagic (*B. panamense, V. lucetia*) and demersal species (*S. ovale*), might have its origin on the spawning of those species mainly to the south of the front; their eggs and larvae would be horizontally limited by the front and vertically by the pycnocline. Previous ichthyoplankton studies in the southern Gulf of California (e.g., Aceves-Medina et al., 2004; Sánchez-Velasco et al., 2006) found during summer a larval assemblage with composition and dominance similar to those of our Warm-frontal assemblage. This suggests that this community of fish larvae is typical of the southern Gulf, and that the surface thermal–chlorophyll front may be its macroscale northern limit.

The presence of the Warm-frontal assemblage in a few upper layer samples inside the cool zone could be due to the evolution of the front position (Fig. 2), and its associated ecosystem, at tidal and subtidal scales in relation to the sampling grid. It may also be that the surface front is not impermeable to surface properties (such as fish larvae) at submesoscale scales (e.g. due to frontal instabilities); the presence of these phenomena in the frontal region is evident in the satellite images presented here and elsewhere (e.g., Paden et al., 1991; Sánchez-Velasco et al., 2009).

The Deep assemblage, located under the pycnocline in the warm side of the front, was dominated by larvae of mesopelagic species such as *B. panamense* and *V. lucetia*. These larvae were also present in the Warm-frontal assemblage, which means that the adults of mesopelagic species spawned through the water column, so their larvae were part of two planktonic habitats separated by the pycnocline. There are very few studies on the migratory capacity of fish larvae, but it is known that the mesopelagic larvae have higher vertical mobility than the others species (e.g., Watanabe et al., 2002); therefore it is also possible that the mesopelagic larvae, especially those in the postflexion stage, could cross the pycnocline. The larval dominance of mesopelagic species through the water column has also been observed in other general studies on the vertical distribution of fish larvae during the stratification period in the Tropical Pacific (Loeb and Nichols, 1984) and in the California Current (Moser and Smith, 1993).

The absence of the Deep assemblage under the pycnocline in the cool side of the front, and the record of samples that did not contain any fish larvae, coincided with the presence of the subsurface salinity maximum intrusion (Fig. 4b), which could be functioning as a horizontal boundary for the mesopelagic larvae that conform the Deep assemblage. This result indicates that the thermohaline circulation, via water mass transfer, affects the distribution of larval assemblages. In addition, the numerical model suggests a blockage of the northward subsurface flow at the 100–150 m layer (Fig. 6c) and at deeper layers (not shown); this reflects the complex oceanography of the zone affecting the larval fish distribution.

4.2. Front-fish larvae relationships in other ecosystems

Studies focusing on the interactions between fish larvae and frontal areas with different sampling scales in diverse regions of the world agree that the frontal areas act as boundaries or barriers restricting larval dispersal, thus contributing to larval survival (e.g., Fortier and Gagne, 1990; Iles and Sinclair, 1982). However, the physical–biological interactions change with the type of front, and a general pattern has not yet been defined. For example Moser and Smith (1993) and Sassa et al. (2007) found different larval composition on either side of semi-permanent oceanic fronts in the California Current and the northwestern Pacific, associated with the different water masses; Sabatés and Olivar (1996) and Wishner et al. (2006) recorded boundaries of the distribution of the costal and/or neritic species in frontal areas on the shelf in the northwestern Mediterranean (salinity front) and the northwestern Atlantic (tidal front). However, the spatial scale of their sampling scheme did not have the fine resolution needed to reveal in detail the vertical processes that occur at the frontal zones.

In the present study we used closely-spaced observations to establish that a deepwater tidal-mixing surface thermal/chlorophyll front had a profound effect on LFAs distribution in the surface layer, while the southward intrusion of maximum-salinity water from the northern Gulf bounded the LFAs distribution in the deeper layer under the pycnocline. However, more work is needed to further our understanding of the three-dimensional evolution of the physical–biological interactions associated with fronts and their differentiating effects on the fish species during their larval development. The definition of planktonic habitats may help to explain the survival strategies of the LFAs that are generated in these complex structures around of the world.

5. Conclusions

We have provided a detailed description of the three-dimensional hydrographic structure and larval fish distribution in the thermal/chlorophyll frontal area in the southern side of the midriff archipelago region of the Gulf of California during August 2005. The three LFAs defined by the Bray–Curtis dissimilarity index were bound differently by hydrographic structures and circulation during the sampling period: (1) The surface thermal/chlorophyll front and the circulation that it induced had a profound effect on the formation of planktonic habitats and therefore on the distribution of the LFAs in the surface layer, maintaining in the top 50 m of the cool side of the front an LFA (Cool-frontal) with the lowest larval abundance and low taxa number, while keeping in the warm side of the front a LFA (Warm-frontal) with the highest mean larval abundance and number of taxa, composed of epipelagic, mesopelagic and demersal species; (2) The hydrographic distribution and the seasonal circulation kept to the southern region of the sampled area a LFA (Deep) with low larval abundance and formed by mesopelagic species; (3) The high-salinity, low-chlorophyll water in the upper layers of the most northerly station, and the subsurface (50–120 m) salinity maximum (35.3) to the north of the front did not contain any fish larvae. The latter suggests that hydrographic processes associated with the Gulf's seasonal and thermohaline circulation can affect the distribution of fish larvae by generating different planktonic habitats.

Acknowledgements

This work was made possible thanks to the financial support of SEP-CONACyT (contracts SEP2004-C01-46349 and 44055), CGPI-Instituto Politécnico Nacional (projects SIP 20090578 and SIP

20080496), and CONACYT contract D41881-F. Thanks to Alberto Amador and Víctor Godínez (CICESE) for their support in the physical data processing, to Carlos Cabrera (CICESE) for his support with satellite image processing and to Arturo Ocampo (CICESE) and Alma Rosa Padilla Pilotze (Instituto de Ciencias del Mar y Limonología, Universidad Nacional Autónoma de México) for her support in the sampling. Thanks to Mayra Pazos and the Drifter Data Assembly Center (GDP/NOAA) for drifter data handling.

Supplementary data

Annex 1. Dendrogram of groups of strata defined by the Bray–Curtis dissimilarly index and the flexible agglomerative method from fish larvae data collected in the midriff archipelago region of the Gulf of California in August 2005. Supplementary data associated with this article can be found, in the online version, at doi:10.1016/j.ecss.2009.09.010.

References

Aceves-Medina, G., Hinojosa-Medina, A., Jiménez-Rosenberg, S.P.A., Funes-Rodríguez, R., Saldierna-Rodríguez, R., 2004. Fish larvae assemblages in the Gulf of California. Journal of Fish Biology 65, 832–847.

Álvarez-Borrego, S., Lara-Lara, R., 1991. The physical environment and primary productivity of the Gulf of California. In: Simoneit, B.R.T., Dauplin, J.P. (Eds.), Gulf and peninsular provinces of the Californias, 47. American Association of Petroleum Geologists, Memoir, pp. 555–567.

Argote, M.L., Amador, A., Lavín, M.F., Hunter, J.R., 1995. Tidal dissipation and stratification in the Gulf of California. Journal of Geophysical Research 100, 16103–16118.

Avalos-García, C., Sánchez-Velasco, L., Shirasago, B., 2003. Larval fish assemblages in the Gulf of California and their relation to hydrographic variability (autumn 1997–summer 1998). Bulletin of Marine Science 72, 63–76.

Bray, J.R., Curtis, J.T., 1957. An ordination of the upland forest communities of Southern Wisconsin. Ecological Monographs 27, 325–349.

Cortés-Lara, M.C., Álvarez-Borrego, S., Giles-Guzmán, A., 1999. Efecto de la mezcla vertical sobre la distribución de nutrientes y fitoplancton en el Golfo de California en verano. Revista de la Sociedad Mexicana de Historia Natural 49, 193–206.

Espinosa-Fuentes, M.L., Flores-Coto, C., 2004. Cross-shelf and vertical structure of ichthyoplankton assemblages in continental shelf waters of the Southern Gulf of Mexico. Estuarine Coastal and Shelf Science 59, 333–352.

Field, J.G., Clarke, K.R., Warwick, R.M., 1982. A practical strategy for analyzing multispecies distribution patterns. Marine Ecology Progress Series 8, 37–52.

Fortier, L., Gagne, J.A., 1990. Larval herring dispersion, growth and survival in the St. Lawrence estuary: match–mismatch or membership/vagrancy? Canadian Journal of Fisheries and Aquatic Sciences 47, 1898–1912.

Green-Ruiz, Y., Hinojosa-Corona, A., 1997. Study of the spawning area of the Northern anchovy in the Gulf of California from 1990 to 1994, using satellite images of sea surface temperature. Journal of Plankton Research 19, 957–968.

Hansen, D., Poulain, P.M., 1996. Quality control and interpolations of WOCE-TOGA drifter data. Journal of Atmospheric and Oceanic Technology 13, 900–909.

Iles, T.D., Sinclair, M., 1982. Atlantic herring: stock discreteness and abundance. Science 215, 627–633.

Kramer, D., Kalin, M.J., Stevens, E.G., Thrailkill, J.R., Zweifel, J.R., 1972. Collecting and processing data on fish eggs and larvae in the California Current region. NOAA Technical Report NMFS CIRC-370, pp. 38.

Lavín, M.F., Marinone, S.G., 2003. An overview of the Physical Oceanography of the Gulf of California. In: Velasco Fuentes, O.U., Sheinbaum, J., Ochoa de la Torre, J.L. (Eds.), Nonlinear Processes in Geophysical Fluid Dynamics. Kluwer Academic Publishers, Dordrecht, Netherlands, ISBN 1-4020-1589-5, pp. 173–204.

Loeb, V.J., Nichols, A., 1984. Vertical distribution and composition of ichthyoplankton and invertebrate zooplankton assemblages in the eastern tropical Pacific. Biología Pesquera 13, 39–66.

Marinone, S.G., 2003. A three-dimensional model of the mean and seasonal circulation of the Gulf of California. Journal of Geophysical Research 108 (C(10)). doi:10.1029/2002JC001720 3325.

Marinone, S.G., Lavín, M.F., 2003. Residual circulation and mixing in the large islands region of the central Gulf of California. In: Velasco Fuentes, O.U., Sheinbaum, J., Ochoa de la Torre, J.L. (Eds.), Nonlinear Processes in Geophysical Fluid Dynamics. Kluwer Academic Publishers, Dordrecht, Netherlands, ISBN 1-4020-1589-5, pp. 213–236.

Mateos, E., Marinone, S.G., Lavín, M.F., 2006. Role of tides and mixing in the formation of an anticyclonic gyre in San Pedro Mártir Basin, Gulf of California. Deep-Sea Research II 53, 60–76. doi:10.016/j.dsr2.2005.07.010.

Moser, H.G., Smith, P.E., 1993. Larval fish assemblages of the California Current region and their horizontal and vertical distributions across a front. Bulletin of Marine Science 53, 645–691.

Moser, H.G., 1996. The early stages of fishes in the California Current Region, 33. CalCOFI Atlas, pp. 1505.

Okazaki, Y., Nakata, H., 2007. Effect of the mesoscale hydrographic features on larval fish distribution across the shelf break of East China Sea. Continental Shelf Research 27, 1616–1628.

Paden, C.A., Abbott, M.R., Winant, C.C., 1991. Tidal and atmospheric forcing of the upper ocean in the Gulf of California 1. Sea surface temperature variability. Journal of Geophysical Research 96, 337–359.

Peguero-Icaza, M., Sánchez-Velasco, L., Lavín, M.F., Marinone, S.G., 2008. Larval fish assemblages, hydrography and circulation in the Gulf of California. Estuarine Coastal and Shelf Science 79, 277–288.

Sabatés, A., Olivar, M.P., 1996. Variation of larval fish distributions associated with variability in the location of a shelf–slope front. Marine Ecology Progress Series 135, 11–20.

Sánchez-Velasco, L., Jiménez-Rosenberg, S.P.A., Lavín, M.F., 2007. Vertical distribution of fish larvae and its relation with water column structure in the SW of the Gulf of California. Pacific Science 61, 533–548.

Sánchez-Velasco, L., Beier, E., Avalos-García, C., Lavín, M.F., 2006. Larval fish assemblages and geostrophic circulation in Bahía de La Paz and the surrounding southwestern region of the Gulf of California. Journal of Plankton Research 28, 1081–1098.

Sánchez-Velasco, L., Avalos-García, C., Rentería-Cano, E., Shirasago, B., 2004. Fish larvae abundance and distribution in the central Gulf of California during strong environmental changes (El Niño 1997–1998 and la Niña 1998–1999). Deep-Sea Research II 51, 711–722.

Sánchez-Velasco, L., Lavín, M.F., Peguero-Icaza, M., León-Chávez, C.A., Contreras-Catala, F., Gutiérrez-Palacios, I.V., Godínez, V.M., 2009. Seasonal changes in larval fish assemblages in a semi-enclosed sea (Gulf of California). Continental Shelf Research, 1697–1710.

Santamaría-del-Angel, E., Álvarez-Borrego, S., Muller-Karger, F.E., 1994. The 1982–1984 El Niño in the Gulf of California as seen in coastal zone color scanner imagery. Journal of Geophysical Research 99, 7427–7431.

Sassa, C., Kawaguchi, K., Taki, K., 2007. Larval mesopelagic fish assemblages in the Kuroshio–Oyashio transition region of the western North Pacific. Marine Biology 150, 1403–1415.

Siegel, S., Castellón, N.J., 1988. Non-parametric Statistics for the Behavioral Sciences. McGraw-Hill International Editions, Statistics Series, pp. 399.

Simpson, J.H., Souza, A.J., Lavín, M.F., 1994. Tidal mixing in the Gulf of California. In: Beven, K., Chatwin, P., Millbank, J. (Eds.), Mixing and Transport in the Environment. Cath Allen Memorial Volume. Lancaster University, John Wiley, pp. 169–182.

Smith, P.E., Richardson, S.L., 1979. Técnicas modelo para prospecciones de huevos y larvas de peces pelágicos. FAO, Documentos Técnicos de Pesca No175, FIR/T175, pp. 107.

Sokal, R.R., Rohlf, F.J., 1985. Biometría. Glume. Barcelona, Spain, pp. 587.

Sokal, R.R., Sneath, P.H., 1963. Principles of Numerical Taxonomy. Freeman, San Francisco, pp. 359.

Sournia, A., 1994. Pelagic biogeography and fronts. Progress in Oceanography 34, 109–120.

Watanabe, H., Kawaguchi, K., Hayashi, A., 2002. Feeding habitats of juvenile surface-migratory myctophid fishes (family Myctophidae) in the Kuroshio region of the western North Pacific. Marine Ecology Progress Series 236, 263–272.

Wishner, K.F., Outram, D., Ullman, D.S., 2006. Zooplankton distributions and transport across the northeastern tidal front of George Bank. Deep-Sea Research II 53, 2570–2596.